Smart Structures and Systems, *Vol. 28, No. 1 (2021) 43-53*
https://doi.org/10.12989/sss.2021.28.1.043

Investigation on modulation of multi-frequency ultrasonic waves in structures with quadratic nonlinearity

Hamid Salehi [1a], Mahnaz Shamshirsaz*[1] and Mohammad Mohammadi Aghdam [2b]

[1] *New Technologies Research Center, Amirkabir University of Technology, Tehran, Iran*
[2] *Mechanical Engineering Department, Amirkabir University of Technology, Tehran, Iran*

(*Received March 14, 2020, Revised November 28, 2020, Accepted April 4 2021*)

Abstract. In this study, the modulation of multiple frequency content of a single ultrasonic wave in nonlinear structures is investigated analytically, numerically and experimentally. An experimental technique is proposed based on nonlinear lamb wave propagation in aluminum bars using piezoelectric wafer active sensors (PWAS) to study intrinsic nonlinearity of structures. First, a one-dimensional analytical procedure is developed to study the modulation of one dimensional wave with multiple-frequency content in isotropic medium with quadratic nonlinearity. This procedure is implemented to study modulation of frequency contents of a well-known tone burst signal in nonlinear medium. Then, predictions obtained by the proposed analytical procedure are compared with the results of finite element model, which show strong correlations. The experimental and analytical results reveal that in excitation with a train of tone burst, due to frequency modulation, some new harmonics including a strong sub harmonic generation with frequency of f_0/N_p appear in the response. The amplitude of this harmonic is even higher than common second harmonic generation ($2f_0$). This can be seen in the experimental results when the excitation frequencies are correctly selected. Finally, it is explained that, why the new sub harmonic generation is less affected by the nonlinearity induced by the excitation system.

Keywords: distributed damage; frequency modulation; nonlinear medium; PWAS; ultrasonic waves

1. Introduction

Continuous accumulation of fatigue damage gradually deteriorates different types of structures and machine parts. Nondestructive inspection (NDI) and Structural health monitoring (SHM) technologies are widely investigated to detect fatigue damage in structures. One of the most popular methods of non-destructive testing is the ultrasonic technique. Among the different features extracted from ultrasonic testing, such as time of flight (Yu and Giurgiutiu 2005) and electromechanical impedance (Karayannis *et al*. 2015, Rajabi *et al*. 2017), nonlinear features show greater sensitivity to small defects which can be used to detect fatigue damages in early stages (Deng and Pei 2007, Prawin and Rao 2018). Depending on the principle of detection, nonlinear ultrasonic methods can be divided into higher and sub harmonic generations (Ginzburg *et al*. 2017, Ding *et al*. 2018, Masurkar *et al*. 2018, Li *et al*. 2020), resonance frequency shift (Solodov 2014), vibro-acoustic modulation (Zhang *et al*. 2017a, Klepka *et al*. 2019, Singh *et al*. 2019) and wave mixing methods (Chen *et al*. 2014, Jingpin *et al*. 2017a, Ding *et al*. 2020). Among these methods, harmonic generations are widely used by many researchers to evaluate early damages in structure experimentally and analytically (Cantrell 2003, Deng 2009, Pruell *et al*. 2009, Ding *et al*. 2018, Masurkar *et al*. 2018). One of the drawbacks of the harmonic generation method is inevitable distortions in the transmitting/receiving system and coupling media which add considerable higher harmonics to exciting signal (Jingpin *et al*. 2015). In practice, it is difficult to separate harmonic generations due to nonlinearity of testing system from structural nonlinearity. To overcome this problem, the method of vibro-acoustic modulation and wave mixing are proposed by some researchers. Based on these techniques, if two waves with different frequencies interact each other through a nonlinear medium, these nonlinearities can lead to generation of some new waves with different frequencies (Jingpin *et al*. 2017a). The amplitude of these new resonance waves is related to the nonlinearity of materials and structures and is less sensitive to nonlinearities in the measurement system (Croxford *et al*. 2009). Also, these techniques provide flexibility in selecting wave modes, frequencies, and propagation directions (Croxford *et al*. 2009). Vibro-acoustic wave modulation technique is based on the modulation of a strong low-frequency vibration, called pumping wave, on a high-frequency acoustic wave, called probing wave (Zhang *et al*. 2017a). The technique is successfully applied to identify different structural defects like local (Liu *et al*. 2016, Klepka *et al*. 2019) and micro cracks (Huifeng *et al*. 2019) of metallic structures, impact damages (Dao *et al*. 2017) and delamination in composite structures (Singh *et al*. 2019). While vibro-acoustic modulation is mainly used for experimental observation of

*Corresponding author, Professor,
E-mail: shamshir@aut.ac.ir
[a] Ph.D. Student, E-mail: hamidsalehi@aut.ac.ir
[b] Professor, E-mail: aghdam@aut.ac.ir

ISSN: 1738-1584 (Print), 1738-1991 (Online)

non-classical material nonlinearities, there is considerable reports on using wave mixing technique to study classical nonlinearity of materials such as evenly distributed damages in structures. In this method, two intersecting ultrasonic waves interact with material nonlinearity and therefore, other waves are generated with frequencies equal to the sum and difference of primary frequencies through the structure (Jingpin *et al*. 2017b). In the case where two intersecting waves propagate in the same or opposite directions, the method is called collinear wave mixing. Other the other hand, the non-collinear wave mixing is used when two intersecting waves propagate in nonparallel but coplanar directions (Jingpin *et al*. 2017b). Liu *et al*. (2012) applied a collinear wave mixing method to study plastic deformation and fatigue damages of Al-6061 alloys. Tang *et al*. (2014) developed a scanning method based on collinear mixing to detect localized plastic deformation. Chen *et al*. (2014) derived a set of necessary conditions for generating resonant waves from two propagating time-harmonic plane waves and obtained closed-form analytical solutions for resonant waves generated by two collinearly propagating sinusoidal pulses. Zhao *et al*. (2015) investigated the frequency deviation during imperfect resonant conditions through FEM simulations and experimental measurements using a one-way mixing technique. Also, many researchers have used non-collinear wave-mixing method for detection of structural damages in early stages. Croxford *et al*. (2009) studied the application of a non-collinear mixing technique for the assessment of plasticity and fatigue damage. Demcenko *et al*. (2012) used non-collinear wave mixing to study physical aging of polyvinyl chloride. Zhang *et al*. (2016) developed two analytical models for estimating the mixing efficiency of two non-collinear shear waves at an imperfect interface. Jingpin *et al*. (2017b) applied non-collinear technique to evaluate fatigue cracks in steel beams.

It is generally known that the nonlinear behavior of electronic instruments appears mainly in the form of higher harmonics and electronic instruments rarely produce subharmonics (Zhang *et al*. 2017b, Jhang 2009, Jeong and Barnard 2011). Therefore, sub harmonic components resulting from frequency modulation and wave mixing techniques are more reliable for detecting structural nonlinearity comparing to higher harmonic generations which is strongly affected by piezoelectric and electronic devices nonlinearities (Jeong and Barnard 2011).

According to some advantages of lamb waves including long distance propagation within plate and shell structures and ability to access hidden section of structures (Peng *et al*. 2006, Ding *et al*. 2018), some researches are carried out based on lamb wave mixing technique (Jingpin *et al*. 2017a, Li *et al*. 2018, Metya *et al*. 2018, Ding *et al*. 2020, Sun *et al*. 2019). Metya *et al*. (2018) used nonlinear lamb wave mixing technique to assess the localized deformation of steel samples during creep. Ding *et al*. (2020) numerically studied nonlinear behavior of thin plates with randomly distributed micro-cracks using one-way Lamb mixing method. Sun *et al*. (2019) applied interaction of counter-propagating Lamb waves to detect and localize micro cracks in plates. Li *et al*. (2018) investigated propagation of Lamb waves in thin plates with quadratic nonlinearity by one way mixing method using numerical simulations. They showed that due to frequency deviation, the waveform of the mixing wave changes significantly from a regular diamond shape to tone burst trains. Jingpin *et al*. (2017a) applied nonlinear Lamb wave-mixing to detect micro-cracks in plates. They combined two Hanning windowed tone burst signals with different central frequencies to study the modulation of main frequencies of these signals through the cracked plate. It is well known that frequency spectrum of any time limited signals covers many frequencies. According to analytical solution of nonlinear wave equation, multi frequency content of any wave can modulate each other during propagation of wave through the nonlinear medium. However, many authors used two separate exciting tools for wave modulation study.

In this paper, the propagation of multi frequency ultrasonic waves is studied in nonlinear medium using analytical, numerical and experimental methods. It is shown that a general solution can be obtained for modulation of multiple-frequency exciting signals. Hence, the modulation of three frequency contents of a tone burst signal is investigated using proposed analytical procedure and numerical method. Finally, the proposed procedure for wave modulation is used for experimental study of lamb wave modulation through an aluminum bar with intrinsic nonlinearity. For the first time, piezoelectric wafer active sensors (PWAS) are employed for considering intrinsic nonlinearity of metals.

2. Considering nonlinear wave equations using Laplace transforms

One-dimensional nonlinear wave problem is studied by many authors (Hikata *et al*. 1965, Zhou *et al*. 2012, Fierro and Meo 2015). The governing equations for this problem is derived in terms of displacement, using dynamic equation of motion and nonlinear hook's low (Zhou *et al*. 2012) as

$$E\frac{\partial^2 u(x,t)}{\partial x^2}+E\beta\frac{\partial^2 u(x,t)}{\partial x^2}\frac{\partial U(x.t)}{\partial x}-\rho\frac{\partial^2 u(x,t)}{\partial t^2}=0 \tag{1}$$

in which E is linear modulus of elasticity, ρ is density and β is called second-order nonlinear elastic coefficient (Xiang *et al*. 2014). Since, nonlinear equations generally have no exact analytical solutions, some semi-analytical methods are used to obtain approximate closed form solutions for these problems. Using perturbation method Eq. (1) can be converted to series of linear equation

$$c^2\frac{\partial^2 u_0}{\partial x^2}-\frac{\partial^2 u_0}{\partial t^2}=0 \tag{2a}$$

$$c^2\frac{\partial^2 u_1}{\partial x^2}-\frac{\partial^2 u_1}{\partial t^2}=c^2\beta\frac{\partial^2 u_0}{\partial x^2}\frac{\partial u_0}{\partial x} \tag{2b}$$

$$c^2\frac{\partial^2 u_2}{\partial x^2}-\frac{\partial^2 u_2}{\partial t^2}=c^2\beta\left\{\frac{\partial^2 u_0}{\partial x^2}\frac{\partial u_1}{\partial x}+\frac{\partial^2 u_1}{\partial x^2}\frac{\partial u_0}{\partial x}\right\} \tag{2c}$$

and so on. In these equations $c(\sqrt{E/\rho})$ is speed of sound. The Eq. (2a) is the famous wave equation in the linear medium. The next equations represent the deviation of the general solution from the linear part. These equations can be solved for different boundary and initial conditions. Semi-infinite wave problem can help to better understanding of NDI process using ultrasonic waves. In this paper this problem is solved using Laplace transforms. Consider a semi-infinite rod which is excited at the beginning by proper harmonic load. Therefore, an ultrasonic wave is formed and propagates through the rod. Prior to excitation, the rod is free from any stress and displacement. There is no reflection from the end of rod due to semi-infinite assumption. Therefore, initial and boundary conditions can be written as

$$u(x,0) = \frac{\partial u(x,0)}{\partial t} = 0, \quad u(0,\mathrm{t}) = H(t)X_0 \sin(\omega t) \tag{3}$$

in which $H(t)$ is Heaviside function, X_0 is amplitude of excitation and ω is its frequency. Typically, in the perturbation method, non-zero boundary conditions assumed to be specific to the first equation (Eq. 2a). Thus, the other equations will have zero boundary conditions. Using Laplace transform the solution for Eq. (2a) will be

$$u_0(x,t) = X_0 H\left(t-\frac{x}{c}\right)\sin\left(\omega\left(t-\frac{x}{c}\right)\right) \tag{4}$$

This is the well-known solution of linear wave problem. The second relation in Eq. (2) is a non-homogeneous PDE. Its non-homogeneity is related to Eq. (4). Therefore, using the result of Eq. (4), Eq. (2b) can be rewritten as

$$\begin{aligned} &c^2\frac{\partial^2 u_1}{\partial x^2} - \frac{\partial^2 u_1}{\partial t^2} \\ &= \beta\frac{X_0^2}{2c}\left\{\omega^3 H^2\left(t-\frac{x}{c}\right)\sin\left(2\omega\left(t-\frac{x}{c}\right)\right)\right\} \end{aligned} \tag{5}$$

It can be proved that the Laplace transform of the second power of the Heaviside function is the same as simple Heaviside function. Therefore, using Laplace transform for Eq. (5) leads to

$$c^2\frac{\partial^2 U_1}{\partial x^2} - s^2 U_1 = -\beta\left[\frac{X_0^2\omega^4}{2c}\frac{e^{-xs/c}}{s^2+\omega^2}\right] \tag{6}$$

Eq. (6) is a nonhomogeneous ODE with zero boundary condition. The solution to this equation will be

$$\begin{aligned} U_1(x,s) = {} & C_1(s)e^{\frac{-sx}{c}} + C_2(s)e^{\frac{sx}{c}} \\ & - \frac{\beta X_0^2\omega^4 e^{\frac{-sx}{c}}(c+2sx)}{4c^2 s^2(s^2+4\omega^2)} \end{aligned} \tag{7}$$

Using inverse Laplace transform, Eq. (7) can be written as

$$\begin{aligned} u_1(x,t) = {} & H\left(t+\frac{x}{c}\right)c_2\left(t+\frac{x}{c}\right) + H\left(t-\frac{x}{c}\right)c_1\left(t-\frac{x}{c}\right) \\ & + H\left(t-\frac{x}{c}\right)\beta X_0^2\left\{\frac{\omega^2 t}{16c} - \frac{\omega\sin\left(2\omega\left(t-\frac{x}{c}\right)\right)}{32c}\right. \\ & \left. - \frac{x\omega^2\cos\left(2\omega\left(t-\frac{x}{c}\right)\right)}{8c^2} + \frac{\omega^2 x}{8c^2}\right\} \end{aligned} \tag{8}$$

When $t = 0$ and $t \to \infty$, u_1 must be zero. Therefore, c_2 becomes zero and after some calculations for obtaining c_1 we have

$$u_1(x,t) = H\left(t-\frac{x}{c}\right)\left\{\frac{\beta X_0^2\omega^2 x}{8c^2}\langle 1-\cos\left(2\omega(t-\frac{x}{c})\right)\rangle\right\} \tag{9}$$

Eq. (9) is the popular solution that can be seen in many references (Hikata *et al*. 1965, Cantrell 2003). As it can be seen in Hikata *et al*. (1965), the solution of Eq. (2c) leads to harmonics which differ from Eq (9). In addition, the amplitude values related to third stage (Eq. 2c) is much smaller than the second one (Eq. 2b).

The proposed procedure based on Laplace transforms shows that $u_1(x,t)$ can be directly obtained controversy to classical method passing by complex computations presented in literature (Malfense-Fierro 2014, Fierro and Meo 2015, Jingpin *et al*. 2015, 2017a). Specially, this complexity increases intensely when the exciting function contains several harmonics. In such case, each existing harmonics in Eq. (2b) modulates with other ones. Therefore, the number of expressions for the Eq. (5) increases enormously. Since the perturbation method converts a nonlinear equation to some linear equations, in each step the equation is linear and therefore, the superposition can be applied. Using this principle, we will suggest a procedure which is able to provide a general solution for multiple exciting frequencies therefore gain the advantage of simplicity of manipulating.

In the calculation of the right side of Eq. (2b), both sine and cosine functions for u_0 lead to sinusoidal functions. Consequently, for multiple exciting functions, after some calculation, this equation can be written as

$$c^2\frac{\partial^2 u_1}{\partial x^2} - \frac{\partial^2 u_1}{\partial t^2} = \sum_{i=1}^{N} A_i \sin\left(B_i\left(t-\frac{x}{c}\right)\right) \tag{10}$$

where N is the number of sinusoidal terms after the calculation of the second side of Eq. (2b) and A_i and B_i are the related amplitudes and frequencies of these terms. Using the superposition, Eq. (10) can be divided into N separate equations as

$$c^2\frac{\partial^2 u_{1i}}{\partial x^2} - \frac{\partial^2 u_{1i}}{\partial t^2} = A_i \sin\left(B_i\left(t-\frac{x}{c}\right)\right) \tag{11}$$

As mentioned earlier, all equations of (10) have zero boundary conditions $(u_{1i}(0,t)=0)$. Using Laplace transform method, the solution of Eq. (11) can be written as

$$u_{1i}(x,t)=\frac{A_i}{2B_ic}x\left(1-\cos\left(B_i\left(t-\frac{x}{c}\right)\right)\right) \tag{12}$$

And finally, the solution of Eq. (10) for multiple frequency excitations can be expressed as

$$u_1(x,t)=\sum_{i=1}^{N}\frac{A_ix}{2B_ic}\left(1-\cos\left(B_i\left(t-\frac{x}{c}\right)\right)\right) \tag{13}$$

As an example, tone burst signal is a finite duration signal and its frequency spectrum covers a limited band of frequencies. This type of signal is used to concentrate the energy of exciting signal near a central frequency. This work can alleviate the dispersion of dispersive waves like Lamb waves. A typical windowed tone burst signal can be written as

$$\begin{aligned}T=\frac{A_s}{2}\left[H(t)-H\left(t-\frac{N_p}{f_c}\right)\right]\\ \sin(2\pi f_ct)\left(1-cos\left(\frac{2\pi f_ct}{N_{\ p}}\right)\right)\end{aligned} \tag{14}$$

where A_s is amplitude, f_c known as carrier frequency, N_p is the number of peaks in signal and $H(t)$ is Heaviside function. Disregarding Heaviside functions in Eq. (14), the signal will have infinite duration with special repeating shapes. After some calculations and assuming this signal as an exciting function of one-dimensional nonlinear medium in $x=0$, we can write this excitation as

$$\begin{aligned}u_0(0,t)=X_0\left\{\sin(\omega_0t)-\frac{1}{2}\sin\left(\frac{N_p+1}{N_p}\omega_0t\right)\right.\\ \left.-\frac{1}{2}\sin\left(\frac{N_p-1}{N_p}\omega_0t\right)\right\}\end{aligned} \tag{15}$$

where $X_0=A_s/2$ and $\omega_0=2\pi f_c$. As it can be seen, in this case, the windowed tone burst signal contains three separate frequencies. Based on solution of linear wave equation, $u_0(0,t)$ for exciting function of Eq. (15) can be written as

$$\begin{aligned}u_0(x,t)=X_0\left\{\sin\left(\omega_0\left(t-\frac{x}{c}\right)\right)\right.\\ -\frac{1}{2}\sin\left(\frac{N_p+1}{N_p}\omega_0\left(t-\frac{x}{c}\right)\right)\\ \left.-\frac{1}{2}\sin\left(\frac{N_p-1}{N_p}\omega_0\left(t-\frac{x}{c}\right)\right)\right\}\end{aligned} \tag{16}$$

After calculation of right side of Eq. (2b) for Eq. (16) and performing some simplifications, we have

$$\begin{aligned}&c^2\frac{\partial^2u_1}{\partial x^2}-\frac{\partial^2u_1}{\partial t^2}\\ &=-\beta\frac{{\omega_0}^3X_0^2}{2c}\left\{\left(\frac{3{N_p}^2-1)}{2{N_p}^2}\right)sin\left(2\omega_0\left(t-\frac{x}{c}\right)\right)\right.\\ &+\frac{1}{4}\left(\frac{N_p+1}{N_p}\right)^3sin\left(2\omega_0\frac{N_p+1}{N_p}\left(t-\frac{x}{c}\right)\right)\\ &+\frac{1}{4}\left(\frac{N_p-1}{N_p}\right)^3sin\left(2\omega_0\frac{N_p-1}{N_p}\left(t-\frac{x}{c}\right)\right)\\ &-\left(\frac{1}{N_p}\right)sin\left(\frac{\omega_0}{N_p}\left(t-\frac{x}{c}\right)\right)\\ &-\frac{1}{2}\left(\frac{2N_p^2+3N_p+1}{N_p^2}\right)sin\left(\frac{2N_p+1}{N_p}\omega_0\left(t-\frac{x}{c}\right)\right)\\ &-\frac{1}{2}\left(\frac{2N_p^2-3N_p+1}{N_p^2}\right)sin\left(\frac{2N_p-1}{N_p}\omega_0\left(t-\frac{x}{c}\right)\right)\\ &\left.+\frac{1}{2}\left(\frac{N_p^2-1)}{N_p^3}\right)sin\left(\frac{2\omega_0}{N_p}\left(t-\frac{x}{c}\right)\right)\right\}\end{aligned} \tag{17}$$

Using Eq. (13) the solution of Eq. (17) can be written as

$$\begin{aligned}u_1(x.t)=\beta\frac{x{\omega_0}^2X_0^2}{4c^2}\left\{\left(\frac{3N_p^2+1)}{8N_p^2}\right)+cos\left(\frac{\omega_0}{N_p}\left(t-\frac{x}{c}\right)\right)\right.\\ -\frac{1}{4}\left(\frac{(N_p^2-1)}{N_p^2}\right)cos\left(\frac{2\omega_0}{N_p}\left(t-\frac{x}{c}\right)\right)\\ -\frac{1}{8}\left(\frac{N_p-1}{N_p}\right)^2cos\left(2\omega_0\frac{N_p-1}{N_p}\left(t-\frac{x}{c}\right)\right)\\ +\frac{1}{2}\left(\frac{N_p-1}{N_p}\right)cos\left(\frac{2N_p-1}{N_p}\omega_0\left(t-\frac{x}{c}\right)\right)\\ -\left(\frac{3N_p^2-1)}{4N_p^2}\right)cos\left(2\omega_0\left(t-\frac{x}{c}\right)\right)\\ +\frac{1}{2}\left(\frac{N_p+1}{N_p}\right)cos\left(\frac{2N_p+1}{N_p}\omega_0\left(t-\frac{x}{c}\right)\right)\\ \left.-\frac{1}{8}\left(\frac{N_p+1}{N_p}\right)^2cos\left(2\omega_0\frac{N_p+1}{N_p}\left(t-\frac{x}{c}\right)\right)\right\}\end{aligned} \tag{18}$$

As can be seen in these results, six new frequencies appear in the solution due to the modulation of three frequencies of initial signal. It is worthy to mention that all amplitudes of new frequencies except for ω_0/N_p, depends on the value of N_p. Also, among the new frequencies, this frequency has the highest amplitude. Because, modulation of both side bands with main frequency leads to generation of waves with same frequency (ω_0/N_p) and these new waves boosts each other.

In general, the term subharmonic refers to harmonic product of single frequency excitation in nonlinear mediums with hysteresis, crack clapping and some other phenomenon. This subharmonic product usually occurs with the frequency of $f_0/2$ (Jhang 2009). However, in some references this term also is used for lower frequency products of modulation and wave mixing phenomenon (Aslam *et al*. 2020, Lee *et al*. 2014). In the present paper, the term "subharmonic" is used in the latter case.

Table 1 Material properties of aluminum

Property	Symbol	Value	Unit
Density	ρ	2700	kg/m^3
Modulus of elasticity	E	70	GPa
Poisson's ratio	ν	0.33	-
Nonlinearity coefficient	β	14.67	-

3. FE simulation

A one-dimensional Finite Element model is used to solve modulation of different exciting functions in nonlinear medium. This model is generated in ABAQUS/CAE and analyzed using implicit dynamic method. Material nonlinearities are implemented by nonlinear stress–strain relation through a user subroutine UMAT. Mechanical properties of medium are taken from Nagy (Nagy *et al*. 2013). Table 1 shows mechanical properties of aluminum material used in FE and analytical model. As the model of Nagy is two-dimensional, the speed of sound is different from the present one-dimensional model.

1800 T3D3 (3-node quadratic 3-D truss) link element is used to simulate the wave propagation in nonlinear medium. This model is shown in Fig. 1.

Displacements are enforced on the left end of medium to excite longitudinal waves. The other end of wire has free boundary condition. However, due to the length of the one-dimensional medium, during solution time, the wave reflection from the end of wire does not happen. The size of elements and time steps are chosen such that the rules of Eq. (19) be satisfied.

$$\Delta t \leq \frac{1}{20 f_{max}} \;\&\; L_{min} = \frac{\lambda}{10} \tag{19}$$

where f_{max} is the highest frequency which exists in the model and λ is equivalent wave length.

4. Experimental set up and procedure

Generation of one-dimensional ultrasonic wave is difficult in many real structural elements and therefore, their structural health monitoring applications are limited. Hence, lamb waves are used to study the modulation of multi-frequency waves. Fig. 2 shows a schematic diagram of the measurement setup used in this study. Two square cross section aluminum bars equipped with PWAS (PZT-5H ceramics with 0.267 mm thickness) at two ends are used as experiment specimens. Recently, PWAS are extensively used for generating and receiving guided waves for structural health monitoring (Kamas *et al*. 2015, Hong *et al*. 2016, Yang *et al*. 2019). This type of actuator/sensor is very light weight, small and cheap and can be bonded easily on the surface of structures (Zhao *et al*. 2007). Therefore, PWAS are proper tools for online monitoring of structures compared to conventional wedge type transducers used by many authors (Barnard *et al*. 2003, Cantrell 2003, Masurkar *et al*. 2018, Li *et al*. 2020).

The dimensions of specimens are 600 mm × 10 mm × 10 mm and piezoelectric actuators and sensors have the same size of aluminum bar cross section. These PZT wafers are bonded to the ends of specimen using thin layer of suitable adhesive. One of PZT wafers is used as actuator while the other one is used to detect propagated waves through the aluminum bar. Excitation signals are generated by Agilent 33220A waveform generator and amplified by an amplifier. The amplitude of exciting signal is 24 Vpp. The response signals acquired from PZT wafer sensor is directly connected to data acquisition system without amplification to reduce possible harmonic distortion due to amplification. Different abilities of PicoScope software are used to perform a real time output signal processing and recording.

Fig. 3 shows a photo of test specimen and experimental setup. For each experiment, excitation is repeated more than 50 times and average of responses is recorded as tests output.

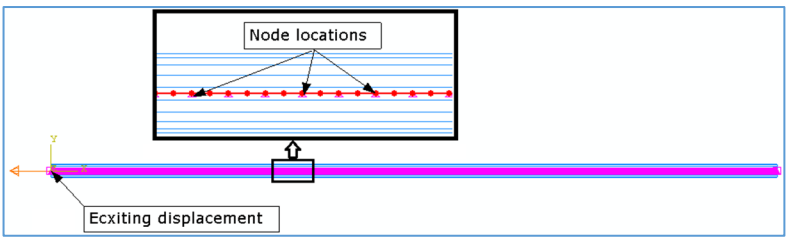

Fig. 1 FE model of one-dimensional nonlinear medium

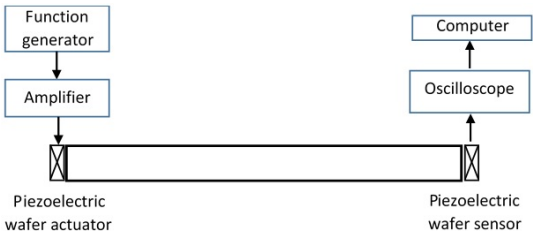

Fig. 2 Schematic representation of experimental set up

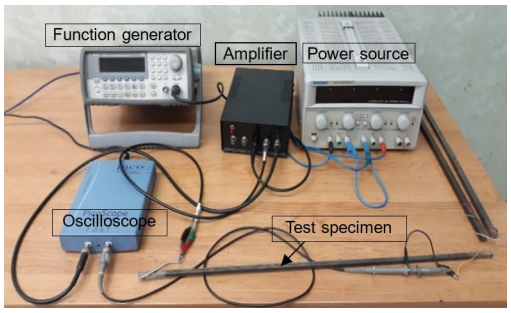

Fig. 3 Experimental setup with an aluminum bar as test specimen

5. Results and discussion

5.1 Analytical and numerical results

A simulation is done using tone burst displacement function and applied to the model at the location x = 0 mm. It is well known that the tone burst has a bell shape in the frequency domain. This is true if, in time domain, the length of tone burst signal is limited to one period ($2\pi N_p/\omega$) of time. If this period doubles, then triple frequencies of Eq. (16) will be revealed in the frequency domain. Logically, the longer the signal is in the time domain, the greater the clarity of these three frequencies will be, which can be clearly seen in Fig. 4. According to Eq. (16) and the results shown in Fig. 4, the values related to excitation are selected as: $X_0 = 500\,nm$, $\omega = 2\pi \times 10^6\,rad/s$, p(total number of excitation displacement cycles) = 20 and $N_p = 5$.

Fig. 5 shows the exciting signal at $x = 0\,mm$ and the response at $x = 50\,mm$. Fundamental harmonics of received signal can be suppressed by simulating numerical model under excitations with positive and negative polarities and then averaging two results (Nagy *et al*. 2013). Using this method, the nonlinear part of received signal of Fig. 5 is depicted in Fig. 6(a). The spectral content of the nonlinear part of response is extracted using Fast Fourier Transforms (FFTs) and depicted in Fig. 6(b). This figure shows that, increasing length of the exciting signal leads to higher accuracy in frequency spectrum.

Fig. 7 shows the frequency spectrum of Fig. 5. As it can be seen, all predicted frequencies in Eq. (18) evidently observable in this figure. The amplitude of different nonlinear features of Fig. 7 are extracted from numerical simulations and compared with presented analytical solution at points $x = 50\,mm$, which are tabulated in Table 2. Two sub harmonics and five higher harmonics are seen by the result presented in Fig. 7 and Table 2. The first sub harmonic demonstrates strong nonlinear amplitude. However, the second one has a weaker amplitude. Three of the five higher harmonics are related to the second harmonic of linear frequencies and two others are due to modulation.

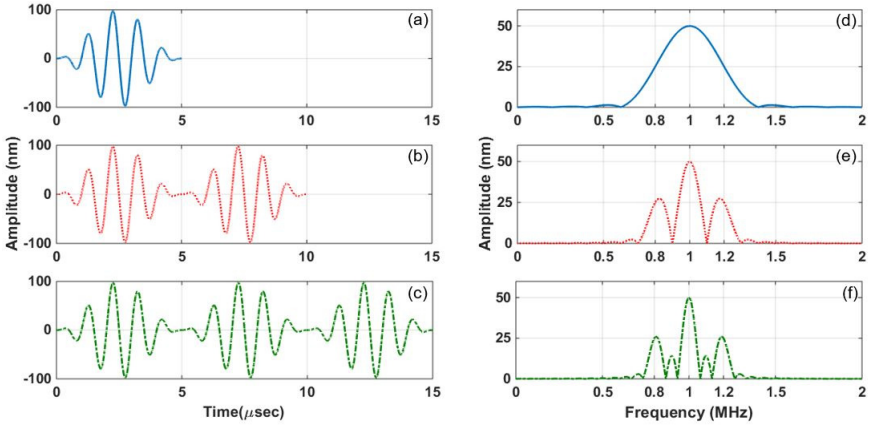

Fig. 4 Effect of time length of signal on frequency spectrum: (a), (b), (c) signals with different time length; (d), (e), (f) FFT of left counterpart signal

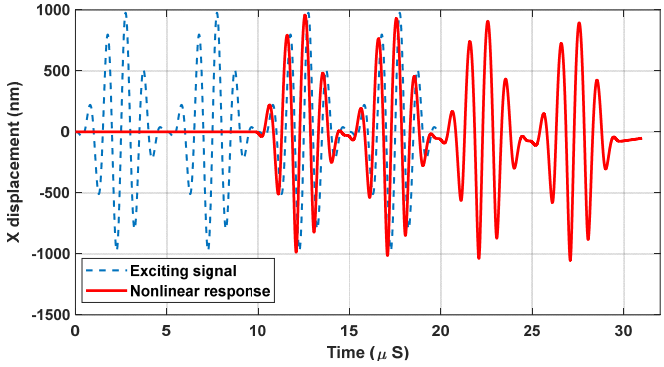

Fig. 5 Excitation and the medium response at x = 50 mm

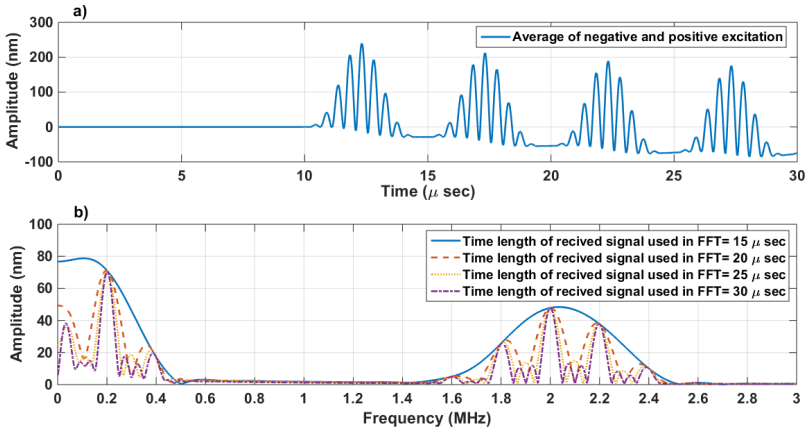

Fig. 6 The effect of signal length on the frequency spectrum of received signal; (a) time domain response; (b) FFT of (a) with different time length

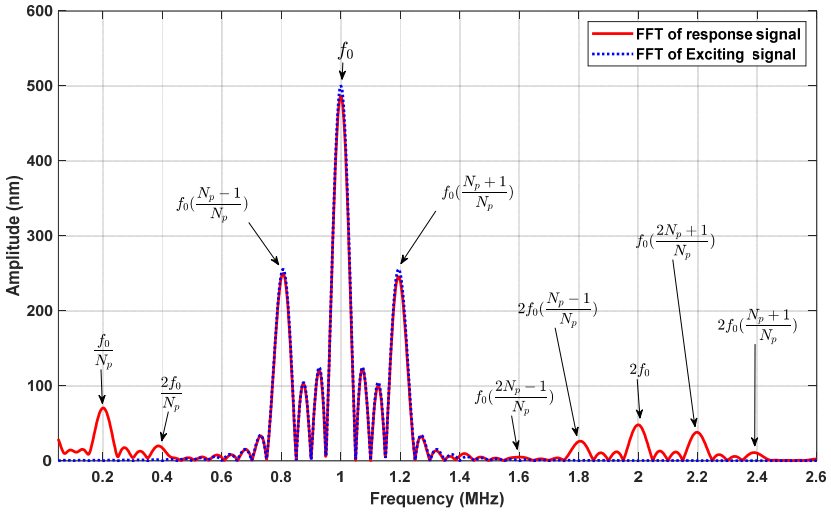

Fig. 7 The appearance of multiple nonlinear frequencies based on FE results given in Fig. 6

Table 2 Amplitude of different features at x = 50 mm

	Analytical solution (nm)	FEM (nm)	Deviation (%)
$0.2\left(\frac{f_0}{N_p}\right)$	69.81	70.83	0.2
$0.4\left(\frac{2f_0}{N_p}\right)$	16.75	16.94	0.4
$1(f_0)$	500	500	0
$1.6\left(2f_0\frac{N_p-1}{N_p}\right)$	5.58	5.65	0.07
$1.8\left(f_0\frac{2N_p-1}{N_p}\right)$	27.92	27.98	0.06
$2(2f_0)$	51.66	51.58	0.08
$2.2\left(f_0\frac{2N_p+1}{N_p}\right)$	41.88	41.81	0.07
$2.4\left(2f_0\frac{N_p+1}{N_p}\right)$	12.57	12.50	0.07

All the results obtained by numerical analysis (Table 2) are in good agreement with the results obtained by proposed analytical procedure summarized in Eq. (18).

In Fig. 8, amplitude changes of these harmonics due to distance change of signal picking point from origin are plotted. As shown in this figure, amplitude changes with a distance from the origin obtained by numerical results are linear as was predicted by Eq. (18).

It should be noted that the location of all harmonics of Eq. (18), except second harmonic of main frequency of excitation signal, are functions of the Np. Thus, changing the Np can change the location of these harmonics in frequency domain. Also, among the new harmonics, the amplitude of ω_0/Np is higher than all harmonics, even at well-known second harmonic.

5.2 Experimental results

As mentioned earlier, the experiment performed in this paper is based on nonlinear lamb wave propagation in structure. However, some predictions by one-dimensional

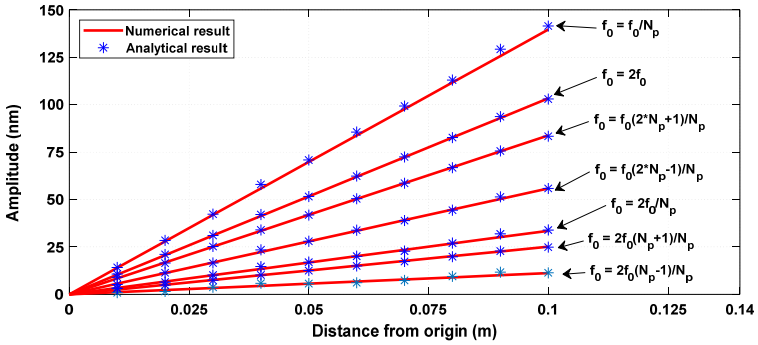

Fig. 8 Amplitude of nonlinear features versus distance from origin

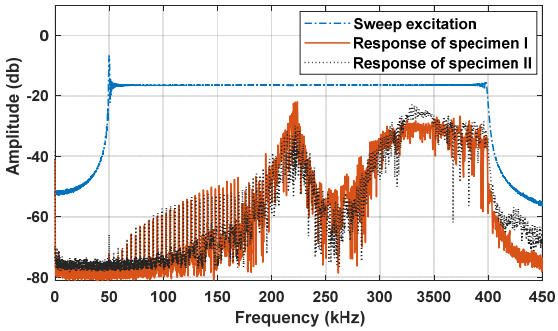

Fig. 9 Response of specimens to sweep excitation

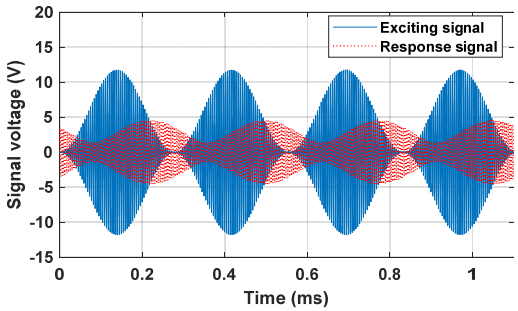

Fig. 10 Train of tone burst signal used for exciting aluminum bar and response signal

wave theory for the lamb wave would not be correct. For example, while the response of two and three-dimensional structures to lamb wave is strongly depend on the excitation frequency, one dimensional wave theory states that the amplitude of output signal is independent of the excitation frequency. Therefore, selecting the correct frequency is very important for nonlinear lamb wave application. A frequency sweep from 50 to 400 kHz with amplitude of 24 Vpp was carried out to select suitable frequencies for tone burst excitation. The response of aluminum bars to this excitation is depicted in Fig. 9. As can be seen in this figure, sweep response of two specimens is similar with each other in resonance frequencies. But, cutting and bonding inaccuracies during PWAS attachment to structure causes some difference on the amplitude of the responses, especially at high frequencies. The highest response amplitude for specimen I is in the frequency range of 210 to 230 kHz and for specimen II is between 320 and 340 kHz. According to Eq. (17) and experimental observations, nonlinear response of structure is affected by linear part.

Therefore, the carrier frequency of tone burst is set on the frequency with highest amplitude. Also, the value of N_p is selected so that the side bands have considerable amplitude. Accordingly, for specimen I, the value of f_0 (carrier frequency) is equal to 220.2 kHz and N_p is equal to 61. Fig. 10 shows time domain plot of the selected excitation and the structural response to this excitation.

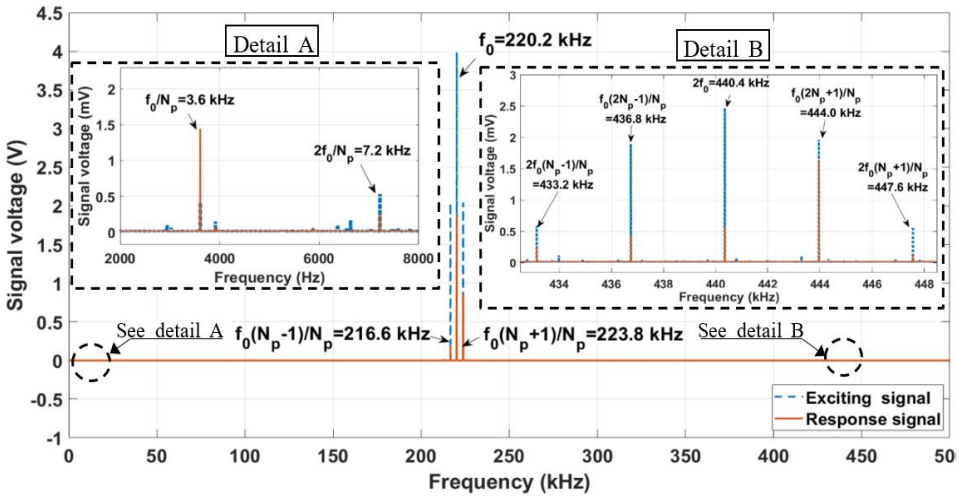

Fig. 11 FFT of tone burst exciting (N_p = 61 and f_0 = 220.2 kHz) and response signals for specimen I

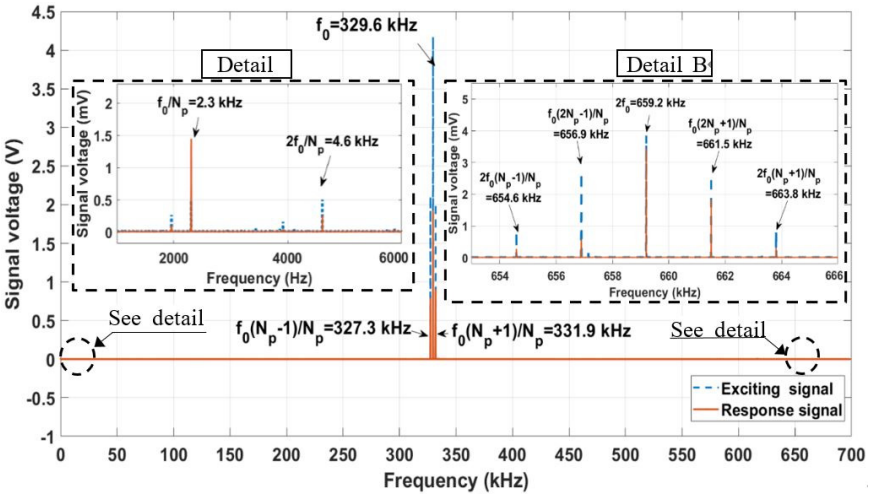

Fig. 12 FFT of tone burst exciting (N_p = 142 and f_0 = 329.6 kHz) and response signals for specimen II

Fig. 11 exhibits the FFT of exciting and response signals. Due to imperfections of excitation system, there are extra harmonics in the excitation signal of Fig. 11.

Moreover, the predicted harmonics of this study can be seen clearly in this figure. Two sub harmonics of f_0/N_p and $2f_0/N_p$ have been generated at frequency points of 3.6 kHz and 7.2 kHz. Also, in accordance with analytical predictions, the amplitude of the first sub harmonic (f_0/N_p) is greater than second one ($2f_0/N_p$). Other harmonics of relation (19), including second harmonic of three main frequencies of tone burst can be seen in Fig. 11.

Another point to mention about second harmonics is that the effect of exciting system on these harmonics is significant. Since the amplitude of the lamb waves is strongly frequency dependent, so the present experimental results cannot exactly cover the analytical predictions about the amplitude of the harmonics.

For specimen II, the value of carrier frequency is set to 329.6 kHz and N_p is equal to 142. The results of this test have been shown in Fig. 12. According the results showed in this figure, all above-mentioned harmonics appears in new frequency points. These frequency changes are proportional to the new value of f_0 and N_p. Also, like previous specimen, for this specimen, the first sub harmonic has strong nonlinearity. According to the results of Figs. 11 and 12, the amplitude of the response in f_0/N_p harmonic is much higher than that of the excitation. This shows that the nonlinear behavior caused by the exciting instruments (refer to Fig. 2) does not play a significant role in creating this harmonic. After sensing PWAS the only electronic tools are data acquisition and signal processing devices. As mentioned in section 1, it is generally known that the nonlinear behavior of electronic instruments appears mainly in the form of higher harmonics. Therefore, it does not seem that the data acquisition signal processing systems can produce such a strong sub harmonic. On the other hand, the repetition of the test for specimen II with different excitation characteristics leads to completely consistent response with the analytical predictions for structural nonlinearity. Therefore, the nonlinearity generated in these two tests is most likely due to wave propagation in the structural nonlinear environment.

Fig. 12 shows that, for specimen II, amplitude of second harmonic in response signal is greater than sub harmonics. This indicates that for the lamb waves, frequency selection has a significant effect on the intensity of nonlinear harmonics.

6. Conclusions

In this study, a new technique is presented for modulation of ultrasonic waves in nonlinear structures using single source excitation. First, an analytical procedure is proposed for considering modulation of multi frequency waves in nonlinear medium using Laplace transforms methods. Using the presented analytical procedure and also numerical simulations, the modulation of the three frequency contents of the well-known windowed tone burst signal was explored. The results show that modulation of each side band frequency with main frequency (carrier frequency) of tone burst signal generates a new strong subharmonic with frequency of f_0/N_p. The experimental tests were performed on aluminum bars to verify the proposed procedure. Experimental results clearly showed the appearance of new sub and higher harmonics due to the modulation of frequency contents of single source ultrasonic wave. According to the results obtained in this study, a single source excitation can be used to modulate frequency contents of excitation signal in nonlinear medium instead of separate excitation methods like vibro-acoustic and common wave mixing techniques.

References

Aslam, M., Bijudas, C.R., Nagarajan, P. and Remanan, M. (2020), "Numerical and Experimental Investigation of Nonlinear Lamb Wave Mixing at Low Frequency", *J. Aerosp. Eng.*, **33**(4), p. 04020037. https://doi.org/10.1061/(ASCE)AS.1943-5525.0001146

Barnard, D.J., Brasche, L.J.H., Raulerson, D. and Degtyar, A.D.

(2003), "Monitoring fatigue damage accumulation with Rayleigh wave harmonic generation measurements", *Review of Progress in QNDE*, **22**, 1393-1400. https://doi.org/10.1063/1.1570294

Cantrell, J.H. (2003), *Fundamentals and Applications of Nonlinear Ultrasonic Nondestructive Evaluation*, CRC Press.

Chen, Z., Tang, G., Zhao, Y., Jacobs, J.L. and Qu, J. (2014), "Mixing of collinear plane wave pulses in elastic solids with quadratic nonlinearity", *J. Acoust. Soc. Am*, **136**, 2389-2404. https://doi.org/10.1121/1.4896567

Croxford, A.J., Wilcox, P.D., Drinkwater, B.W. and Nagy, P.B. (2009), "The use of non-collinear mixing for nonlinear ultrasonic detection of plasticity and fatigue", *J. Acoust. Soc. Am.*, **126**(5), EL117-122. https://doi.org/10.1121/1.3231451

Dao, P.B., Klepka, A., Pieczonka, Ł., Aymerich, F. and Staszewski, W.J. (2017), "Impact damage detection in smart composites using nonlinear acoustics—cointegration analysis for removal of undesired load effect", *Smart Mater. Struct.*, **26**(3), 0350. https://doi.org/10.1088/1361-665X/aa5744

Demcenko, A., Akkerman, R., Nagy, P.B. and Loendersloot, R. (2012), "Non-collinear wave mixing for non-linear ultrasonic detection of physical ageing in PVC", *NDT & E Int.*, **49**, 34-39. https://doi.org/10.1016/j.ndteint.2012.03.005

Deng, M. (2009), "Cumulative second-harmonic generation of Lamb-mode propagation in a solid plate", *J. Appl. Phys.*, **85**, 3051-3058. https://doi.org/10.1063/1.369642

Deng, M. and Pei, J. (2007), "Assessment of accumulated fatigue damage in solid plates using nonlinear Lamb wave approach", *Appl. Phys. Lett.*, **90**(12), 121902. https://doi.org/10.1063/1.2714333

Ding, X., Zhao, Y., Hu, N., Liu, Y., Zhang, J. and Deng, M. (2018), "Experimental and numerical study of nonlinear Lamb waves of a low-frequency S0 mode in plates with quadratic nonlinearity", *Materials*, **11**(11), 2096. https://doi.org/10.3390/ma11112096

Ding, X., Zhao, Y., Deng, M., Shui, G. and Hu, N. (2020), "One-way Lamb mixing method in thin plates with randomly distributed micro-cracks", *Int. J. Mech. Sci.*, **171**, 105371. https://doi.org/10.1016/j.ijmecsci.2019.105371

Fierro, G.P.M. and Meo, M. (2015), "Residual fatigue life estimation using a nonlinear ultrasound modulation method", *Smart Mater. Struct.*, **24**(2), p. 025040. https://doi.org/10.1088/0964-1726/24/2/025040

Ginzburg, D., Ciampa, F., Scarselli, G. and Meo, M. (2017), "SHM of single lap adhesive joints using subharmonic frequencies", *Smart Mater. Struct.*, **26**(10), 105018. https://doi.org/10.1088/1361-665X/aa815c

Hikata, A., Chick, B.B. and Elbaum, C. (1965), "Dislocation contribution to the second harmonic generation of ultrasonic waves", *J. Appl. Phys.*, **36**, 229. https://doi.org/10.1063/1.1713881

Hong, X., Ruan, J., Liu, G., Wang, T., Li, Y. and Song, G. (2016), "Synergetics based damage detection of frame structures using piezoceramic patches", *Smart Struct. Syst., Int. J.*, **17**(2), 167-194. https://doi.org/10.12989/sss.2016.17.2.167

Huifeng, Z., Liuchen, H., Piaopiao, F., Yuebing, W. and Yonggang, C. (2019), "The study of micro-crack localisation based on vibro-acoustic modulation and time reversal method", *Nondestruct. Test. Eval.*, **34**(3), 324-338. https://doi.org/10.1080/10589759.2019.1600687

Jeong, H. and Barnard, D. (2011), "Measurements of sub-and super harmonic waves at the interfaces of fatigue-cracked CT specimen", *J. Korean Soc. Nondestruct. Test.*, **31**(1), 1-10.

Jhang, K.Y. (2009), "Nonlinear ultrasonic techniques for nondestructive assessment of micro damage in material: a review", *Int. J. Precis. Eng. Manuf.*, **10**(1), 123-135. https://doi.org/10.1007/s12541-009-0019-y

Jingpin, J., Junjun, S., Guanghai, L., Bin, W. and Cunfu, H. (2015), "Evaluation of the intergranular corrosion in austenitic stainless steel using collinear wave mixing method", *NDT & E Int.*, **69**, 1-8. https://doi.org/10.1016/j.ndteint.2014.09.001

Jingpin, J., Xiangji, M., Cunfu, H. and Bin, W. (2017a), "Nonlinear Lamb wave-mixing technique for micro-crack detection in plates", *NDT & E Int.*, **85**, 63-71. https://doi.org/10.1016/j.ndteint.2016.10.006

Jingpin, J., Hongtao, L., Cunfu, H. and Bin, W. (2017b), "Fatigue crack evaluation using the non-collinear wave mixing technique", *Smart Mater. Struct.*, **26**(6), 065005. https://doi.org/10.1088/1361-665X/aa6c43

Kamas, T., Poddar, B., Lin, B. and Yu, L.L. (2015), "Assessment of temperature effect in structural health monitoring with piezoelectric wafer active sensors", *Smart Struct. Syst., Int. J.*, **16**(5), 835-851. http://dx.doi.org/10.12989/sss.2015.16.5.835

Karayannis, C.G., Voutetaki, M.E., Chalioris, C.E., Providakis, C.P. and Angeli, G.M. (2015), "Detection of flexural damage stages for RC beams using piezoelectric sensors (PZT)", *Smart Struct. Syst., Int. J.*, **15**(4), 997-1018. https://doi.org/10.12989/sss.2015.15.4.997

Klepka, A., Dziedziech, K., Mrówka, J. and Górski, J. (2019), "Experimental investigation of modulation effects for contact-type interfaces in vibro-acoustic modulation tests", *Struct. Health Monitor.*, 1475921719857624. https://doi.org/10.1177/1475921719857624

Lee, D.J., Cho, Y. and Li, W. (2014), "A feasibility study for Lamb wave mixing nonlinear technique", *AIP Conference Proceedings*, Vol. 1581, No. 1, pp. 662-666, American Institute of Physics. https://doi.org/10.1063/1.4864883

Li, F., Zhao, Y., Cao, P. and Hu, N. (2018), "Mixing of ultrasonic Lamb waves in thin plates with quadratic nonlinearity", *Ultrasonics*, **87**, 33-43. https://doi.org/10.1016/j.ultras.2018.02.005

Li, W., Chen, B. and Cho, Y. (2020), "Nonlinear feature of phase matched Lamb waves in solid plate", *Appl. Acoust.*, **160**, 107124. https://doi.org/10.1016/j.apacoust.2019.107124

Liu, M., Tang, G., Jacobs, L.J. and Qu, J. (2012), "Measuring acoustic nonlinearity parameter using collinear wave mixing", *J. Appl. Phys.*, **112**, 024908. https://doi.org/10.1063/1.4739746

Liu, P., Sohn, H., Yang, S. and Lim, H.J. (2016), "Baseline-free fatigue crack detection based on spectral correlation and nonlinear wave modulation", *Smart Mater. Struct.*, **25**(12), 125034. https://doi.org/10.1088/0964-1726/25/12/125034

Malfense-Fierro, G.P. (2014), "Development of nonlinear ultrasound techniques for multidisciplinary engineering applications", Ph.D. Dissertation; University of Bath, Bath, England.

Masurkar, F., Tse, P. and Yelve, N.P. (2018), "Evaluation of inherent and dislocation induced material nonlinearity in metallic plates using Lamb waves", *Appl. Acoust.*, **136**, 76-85. https://doi.org/10.1016/j.apacoust.2018.02.011

Metya, A.K., Tarafder, S. and Balasubramaniam, K. (2018), "Nonlinear Lamb wave mixing for assessing localized deformation during creep", *NDT & E Int.*, **98**, 89-94. https://doi.org/10.1016/j.ndteint.2018.04.013

Nagy, P.B., Qu, J. and Jacobs, L.J. (2013), "Finite-size effects on the quasistatic displacement pulse in a solid specimen with quadratic nonlinearity", *J. Acoust. Soc. Am.*, **134**(3), 1760-1774. https://doi.org/10.1121/1.4817840

Peng, G., Yuan, S.F. and Xu, X. (2006), "Damage detection on two-dimensional structure based on active Lamb waves", *Smart Struct. Syst., Int. J.*, **2**(2), 171-188. https://doi.org/10.12989/sss.2006.2.2.171

Prawin, J. and Rao, A. (2018), "Detection of nonlinear structural behavior using time-frequency and multivariate analysis", *Smart Struct. Syst., Int. J.*, **22**(6), 711-725. https://doi.org/10.12989/sss.2018.22.6.711

Pruell, C., Kim, J.Y., Qu, J. and Jacobs, L.J. (2009), "Evaluation of fatigue damage using nonlinear guided waves", *Smart Mater. Struct.*, **18**, 035003. https://doi.org/10.1088/0964-1726/18/3/035003

Rajabi, M., Shamshirsaz, M. and Naraghi, M. (2017), "Crack detection in rectangular plate by electromechanical impedance method: modeling and experiment", *Smart Struct. Syst., Int. J.*, **19**(4), 361-369. https://doi.org/10.12989/sss.2017.19.4.361

Singh, A.K., Tan, V.B., Tay, T.E. and Lee, H.P. (2019), "Experimental investigations into nonlinear vibro-acoustics for detection of delaminations in a composite laminate", *J. Nondestruct. Eval. Diagn. Progn. Eng. Syst.*, **2**(1), 011002. https://doi.org/10.1115/1.4041122

Solodov, I. (2014), "Resonant Acoustic Nonlinearity of Defects for Highly-Efficient Nonlinear NDE", *J. Nondestr. Eval.*, **33**(2), 252-262. https://doi.org/10.1007/s10921-014-0229-9

Sun, M., Xiang, Y., Deng, M., Tang, B., Zhu, W. and Xuan, F.Z. (2019), "Experimental and numerical investigations of nonlinear interaction of counter-propagating Lamb waves", *Appl. Phys. Lett.*, **114**(1), 011902. https://doi.org/10.1063/1.5061740

Tang, G., Liu, M., Jacobs, L.J. and Qu, J. (2014), "Detecting localized plastic strain by a scanning collinear wave mixing method", *J. Nondestruct. Eval.*, **33**(2), 196-204. https://doi.org/10.1007/s10921-014-0224-1

Xiang, Y., Deng, M. and Xuan, F.-Z. (2014), "Thermal degradation evaluation of HP40Nb alloy steel after long term service using a nonlinear ultrasonic technique", *J. Nondestruct. Eval.*, **33**, 279-287. https://doi.org/10.1007/s10921-013-0222-8

Yang, S., Jung, J., Liu, P., Lim, H.J., Yi, Y., Sohn, H. and Bae, I.H. (2019), "Ultrasonic wireless sensor development for online fatigue crack detection and failure warning", *Struct. Eng. Mech.*, **69**(4), 407-416. https://doi.org/10.12989/sem.2019.69.4.407

Yu, L. and Giurgiutiu, V. (2005), "Advanced signal processing for enhanced damage detection with piezoelectric wafer active sensors", *Smart Struct. Syst., Int. J.*, **1**(2), 185-215. https://doi.org/10.12989/sss.2005.1.2.185

Zhang, Z., Nagy, P.B. and Hassan, W. (2016), "Analytical and numerical modeling of non-collinear shear wave mixing at an imperfect interface", *Ultrasonics*, **65**, 165-176. https://doi.org/10.1016/j.ultras.2015.09.021

Zhang, Z., Xu, H., Liao, Y., Su, Z. and Xiao, Y. (2017a), "Vibro-acoustic modulation (VAM)-inspired structural integrity monitoring and its applications to bolted composite joints", *Compos. Struct.*, **176**, 505-515. https://doi.org/10.1016/j.compstruct.2017.05.043

Zhang, M., Xiao, L., Qu, W. and Lu, Y. (2017b), "Damage detection of fatigue cracks under nonlinear boundary condition using subharmonic resonance", *Ultrasonics*, **77**, 152-159. https://doi.org/10.1016/j.ultras.2017.02.001

Zhao, X., Gao, H., Zhang, G., Ayhan, B., Yan, F., Kwan, C. and Rose, J. (2007), "Active health monitoring of an aircraft wing with embedded piezoelectric sensor/actuator network: I. Defect detection, localization and growth monitoring", *Smart Mater. Struct.*, **16**(4), 1208. https://doi.org/10.1088/0964-1726/16/4/032

Zhao, Y., Chen, Z., Cao, P. and Qiu, Y. (2015), "Experiment and FEM study of one-way mixing of elastic waves with quadratic nonlinearity", *NDT & E Int.*, **72**, 33-40. https://doi.org/10.1016/j.ndteint.2015.02.004

Zhou, C., Hong, M., Su, Z., Wang, Q. and Cheng, L. (2012), "Evaluation of fatigue cracks using nonlinearities of acousto-ultrasonic waves acquired by an active sensor network", *Smart Mater. Struct.*, **22**(1), 015018. https://doi.org/10.1088/0964-1726/22/1/015018